

Photon Detection with n-Propanol and C₂H₆O Isomers

(Running Title: Photon Detection)

J. A. Lipton-Duffin, A. G. Mark and A. B. McLean*

*Department of Physics, Queen's University,
Kingston, Ontario, Canada, K7L 3N6*

(Dated: September 12, 2002)

Abstract

We demonstrate that a Geiger-Müller-type bandpass photon detector, suitable for inverse photoemission experiments, can be constructed from a MgF₂ entrance window that has a high energy transmission threshold of 10.97eV, and ethanol, a detection gas with an ionization potential of 10.48eV. The photon detector has a mean detection energy of $\hbar\omega_d=(10.89\pm 0.07)$ eV and a bandpass of $\Delta\hbar\omega_d=(0.37\pm 0.05)$ eV. A photon detector can also be constructed from n-propanol/MgF₂ with a mean detection energy of $\hbar\omega_d=(10.76\pm 0.07)$ eV and a bandpass $\Delta\hbar\omega_d=(0.41\pm 0.05)$ eV. These two new detection gas/window combinations have a higher detection energy and a narrower bandpass than the dimethyl ether/MgF₂ detector ($\Delta\hbar\omega_d=(0.71\pm 0.04)$ eV and $\hbar\omega_d=10.60$ eV). Since all three detectors utilize a MgF₂ entrance window, the photon bandpass can be changed straightforwardly by changing the detection gas. For systems that can be easily damaged by electron beams, having the freedom to open up the detector bandpass is an advantage because it can reduce the total electron exposure time.

PACS numbers: 07.07.Df, 51.50.+v, 73.20.-r, 73.90.+f

I. INTRODUCTION

Since the iodine Geiger-Müller (GM) photon detector was first used by Dose and coworkers¹⁻³, GM detectors have played an important role in the development of inverse photoemission as a spectroscopy of unoccupied states^{2,4-6}. The ionization potential (IP) of iodine gas (9.28 ± 0.02)eV⁷ can be matched to the high energy transmission threshold of CaF₂ windows 10.08eV⁸ to produce a medium resolution detector with a bandpass (FWHM) of $\Delta\hbar\omega_d = 0.607$ eV centered on the mean detection energy $\hbar\omega_d = 9.57$ eV⁹. Alternatively, it can be matched to the high energy threshold of SrF₂ (9.80eV)¹⁰ to produce a higher resolution detector with $\Delta\hbar\omega_d = 0.265$ eV and $\hbar\omega_d = 9.43$ eV⁹. GM detectors with both CaF₂ and SrF₂ windows have been used with a great degree of success^{2,4-6}.

Other gas/window combinations have been explored¹¹⁻¹³ to find combinations that avoid iodine, because it is corrosive and the sensitivity of the iodine detector can be as large as 8%/°C¹. For example, Prince¹³ measured the transmission function of the dimethyl ether/MgF₂ combination with synchrotron radiation and suggested that this combination could be used in inverse photoemission experiments. Combining the high energy transmission threshold of MgF₂ (10.97eV)⁸ with the ionization potential of dimethyl ether (10.00 \pm 0.02) eV⁷ produces a bandpass $\Delta\hbar\omega_d \approx 0.6$ eV and a mean detection energy of 10.6 eV¹³(we provide a new determination of the bandpass in this paper). Increasing the mean detection energy is an advantage in inverse photoemission experiments because low energy electron sources are space charge limited. If the mean photon detection energy is increased from $\hbar\omega_d$ to $\hbar\omega'_d = \hbar\omega_d + \Delta$, a state with a binding energy of ε_B , measured relative to the vacuum level, can be probed with electrons that have a kinetic energy of $\varepsilon'_K = \varepsilon_K + \Delta$ since

$$\varepsilon_B = \hbar\omega_d - \varepsilon_K = \hbar\omega'_d - \varepsilon'_K. \quad (1)$$

In the above equation ε_K is the kinetic energy of the electron required to probe a state with a binding energy of ε_B using a detector with a mean detection energy of $\hbar\omega_d$. Since the space charge limited maximum current from our electron source¹⁴ is proportional to $\varepsilon_K^{3/2}$, increasing $\hbar\omega_d$ by Δ , from 9.5 to 10.6eV, allows us to increase the electron current by a multiplicative factor of $(1 + \Delta/\varepsilon_K)^{3/2} \approx 18\%$ while retaining the focussing properties of the source.

Following Prince's suggestion, we built a dimethyl ether/MgF₂ detector¹⁵⁻²¹. However,

we found that the detector needed a quench gas to stop the continuous pulsing¹⁶ that is caused by energetic positive ions scattering electrons from the walls of the tube²². The rule of thumb in choosing a quench gas is to find a gas that has a higher molecular weight and a lower ionization potential, to increase the probability of charge transfer collisions between the detection gas and the quench gas²². In our case, choosing a quench gas with a lower ionization potential would not have been particularly helpful as it would have increased the bandpass of the detector. So we chose ethanol, a common quench gas that does stop the continuous pulsing despite violating conventional wisdom on two counts. Ethanol is an isomer of dimethyl ether and its IP ($10.48\pm 0.05\text{eV}$)⁷ is higher than that of dimethyl ether.

The fact that the dimethyl ether/ethanol mixture works so well, combined with the fact that the ionization potential of the quench gas is lower than the high energy transmission threshold of MgF_2 , encouraged us to try ethanol as a detection gas. We were curious to see if, in addition to quenching dimethyl ether, the ethanol was acting as a detection gas. Since the IP of ethanol lies above the IP of dimethyl ether, it is impossible to tell whether the ethanol is being photoionized during the normal operation of the detector. We found that ethanol can indeed be used as a detection gas. This suggests that in addition to quenching dimethyl ether it is also acting as a detection gas. In the remainder of this paper we will present the first results we have obtained with the ethanol/ MgF_2 detector. After our success with ethanol, we also tried using n-propanol. It has an IP intermediate between dimethyl ether and ethanol (10.20eV)⁷ and it can also be used as a detection gas.

The Geiger-Müller detector is illustrated schematically in FIG.1. It consists of a stainless steel tube welded to a 2.75"-1.33" CF (ConFlat) reducing flange. The gas inlets are two 1.33" CF flanges that are mounted at right angles to the tube. The high voltage connection is made to the central electrode using a 1.33" CF Safe High Voltage (SHV) feedthrough. The central electrode is located in the tube by a 0.875" diameter polytetrafluorethylene (PTFE) spacer, which is press-fit into the tube. The spacer prevents the electrode from sagging in the tube under its own weight, as well as preventing it from vibrating. The MgF_2 window is glued onto the front of the tube using UHV-compatible epoxy.

II. THE DETECTION GAS MIXTURES

We list below the gas mixtures that we use in our GM detectors. Apart from the multiplier gas, the pressures that we provide are uncorrected, measured as apparent N_2 pressures using a convectron gauge (Granville Phillips 275 series). In the case of the quench gas we measure the sum of the detection gas and the quench gas. For the multiplier gas we measure the sum of the detection gas, the quench gas (if required) and the multiplier gas.

A. The Ethanol Detector: CH_3CH_2OH

The gas manifold is drawn schematically in FIG.2. The GM tube was filled as follows. A reservoir containing liquid ethanol was pumped on for approximately 5 minutes using a rotary pump (Edwards). The pump was then isolated from the reservoir and 4-way cross, and the ethanol vapor was allowed to leak into the GM plumbing using a variable leak valve (Varian 9515106), until the pressure on the convectron gauge read 1.15 Torr. The reservoir was then isolated, and the manifold was pumped out and flushed with argon. The manifold was then filled with a backpressure of argon (≈ 5 psi), and the leak valve was used to bring the total pressure in the GM line to a reading of 8.5 Torr (corresponding to approximately 100 Torr Ar). The correction factor was obtained from a graph provided by the gauge manufacturer.

B. The n-Propanol Detector: $CH_3(CH_2)OH$

As with the ethanol detector, the uncorrected partial pressure of the n-propanol detection gas was 1.15Torr and the argon multiplier pressure was ≈ 100 Torr. The filling procedure was identical to the one described for the ethanol detector, except that the ethanol reservoir was replaced with a propanol reservoir.

C. The Dimethyl Ether Detector: $(CH_3)_2O$

For the dimethyl ether detector we used the same gas mixture described previously (0.380Torr of dimethyl ether, 1.15Torr of ethanol and ≈ 100 Torr of argon)¹⁶. The tube was filled by backpressuring the manifold with dimethyl ether, then with ethanol and argon,

as outlined for the other two detectors. Both the dimethyl ether and the ethanol partial pressures were measured with the convectron gauge and are uncorrected. As mentioned above, we believe that the ethanol serves both as a quench gas and a detection gas.

III. DETECTION GAS CONDITIONING

When first run, the freshly filled GM tubes require a certain amount of time to warm up²². This involves careful monitoring of pulse behavior and appropriate adjustments to the high voltage bias (HV) to maintain proper operation. After the multiplier gas was added, the HV was slowly increased ($\approx 10\text{V/s}$) until small pulses were visible on the oscilloscope usually around 600 Volts. The HV was then left constant, and the pulses were observed to grow in amplitude, with timescales on the order of 30 seconds. If allowed to continue unchecked, these discharges would eventually become large enough to completely saturate the tube and produce a continuous breakdown. Thus the HV was decreased by 1-2 volts when the pulses became too large. Over a period of approximately two hours the rate of increase in pulse amplitude slowed and stable operation was achieved, with no further adjustments required to the HV.

Proper GM operation may be checked by verifying that the count rates correspond to Poisson counting statistics²². In this case the GM tube was exposed to an intense source of photons (an ionization gauge filament), and we compared the mean counting rate μ to the standard deviation σ . For Poisson statistics we require that $\sigma = \sqrt{\mu}$. If this relation does not hold, it is possible that the tube is not operating in the Geiger-Müller regime, and that suitable adjustments must be made to the HV. It is important that this type of test be done at a constant chamber pressure, as we have found that the flux of detectable UV photons from ionization gauge filaments varies with pressure.

IV. RESULTS

A. Dead and Recovery Times

In FIG.3 we have superimposed a sequence of pulses from the ethanol GM tube so that the envelope of pulse heights can be examined. The pulses were triggered off the rising edge of the $t = 0$ pulse. The inverse photoemission system that we used to collect these pulses

will be described in more detail in a future publication. The pulses were collected using a National Instruments PXI 5120 digital oscilloscope. The recovery of the normalized pulse height as a function of time ($t > \tau_d$) after the initial pulse can be described by a function of form²²

$$h(t) = 1 - \exp\left(\frac{\tau_d - t}{\tau_r}\right). \quad (2)$$

A non-linear least-squares fit to the experimental pulse height recovery curve yielded a recovery time constant of $\tau_r = (150 \pm 10)\mu s$ and a dead time²² of $\tau_d = (145 \pm 10)\mu s$. The dead time is the time between an initial pulse and a second GM pulse regardless of its size²². The recovery time is the time it takes the pulse height to grow to its full size²². The shape of the pulse recovery curve for the n-propanol and the dimethyl ether detector is very similar. However, the dead and recovery times are different and for completeness they are listed in Table 1. Our dead time gating electronics are set to the sum of the dead and recovery time^{15,16}.

In a non-paralyzable model, dead time losses may be computed by using $\delta = nm\tau_d$ where δ is the rate at which counts are lost, n is the true count rate, and m is the measured count rate²². For $\tau_d \approx 200\mu s$ we will have 2%, 5% and 10% losses when n is equal to 100 cps, 260 cps, and 550 cps, respectively.

B. Energy Bandpass

The bandpasses of the detectors were measured using inverse photoemission spectra of a Cu(111) surface. The sharp onset in the unoccupied density of states above the Fermi level serves as a convenient step function that would, if the resolving power was infinite, be only thermally broadened. The FWHM broadening of the Fermi-Dirac distribution function is²³:

$$\Gamma_{FD} = \left(\ln(3 + 2\sqrt{2}) - \ln(3 - 2\sqrt{2})\right) k_B T = 3.53k_B T, \quad (3)$$

and at $T = (297 \pm 3)K$, $\Gamma_{FD} = (90 \pm 1)\text{meV}$.

We have previously determined¹⁵ that the (FWHM) width of the electron energy distribution from our indirectly heated BaO cathodes under normal operating conditions $\Gamma_{\text{SOURCE}} \approx 220\text{meV}$ ^{15,16}. This is in good agreement with the results of others^{5,14,24}.

In FIG.4a we present a spectrum that was collected from Cu(111) (Monocrystals) with the ethanol detector and our Stoffel-Johnson (S-J) style low energy electron gun¹⁴. The gun was placed in normal incidence to allow us to probe the $\bar{\Gamma}$ symmetry point and the electron current was set to $\approx 10\mu A$. The Cu(111) surface has been used previously to determine the energy resolution²⁴ of a refracting monochromator. Differentiating the spectrum in the vicinity of the Fermi edge yields a peak with a FWHM of $\Gamma_{EXP}=(0.42\pm 0.03)eV$, illustrated in FIG.5a. The presence of the Shockley state just above the Fermi level causes the derivative of the spectrum to swing negative above 8.5eV (e.g. Fig.4)²⁴. Consequently, when a Gaussian function is fit to the derivative of the Fermi edge we might expect the FWHM (Γ_{EXP}) to be narrowed. However, Royer et. al.²⁴ found that the width extracted from the derivative of the Fermi edge and the width extracted from the n=1 image states were comparable (0.56 versus 0.55eV). So we have used the uncorrected Gaussian width as a measure of the experimental energy resolution. Our measurements also indicated that, within experimental uncertainty, Γ_{EXP} did not depend upon the intensity of the Shockley state.

Assuming that both Γ_{FD} and Γ_{SOURCE} add in quadrature we can now calculate the bandpass of the detector from the experimental width (Γ_{EXP}):

$$\Delta\hbar\omega_d = \sqrt{\Gamma_{EXP}^2 - \Gamma_{FD}^2 - \Gamma_{SOURCE}^2}. \quad (4)$$

Using the values quoted above, we obtain $\Delta\hbar\omega_d=(0.37\pm 0.05)eV$ for the ethanol detector. In FIG.4b we present a Fermi edge from Cu(111) measured with the propanol detector. FIG.5b shows the edge is slightly broader indicating that the bandpass of this detector is larger. The shift in the Fermi level also indicates that the mean detection energy has moved. A Cu(111) Fermi edge measured with the dimethyl ether detector is presented in FIG.4c. The edge is clearly broader than either the ethanol or n-propanol edges and our estimate of the bandpass (see FIG.5c) places it at $(0.71\pm 0.04)eV$. This is significantly larger than previous estimates ($\approx 0.6eV$)^{13,15,16}.

We previously found¹⁶ that the width of a polycrystalline gold Fermi edge Γ_{EXP} as measured by a solid state bandpass detector (MM1 electron multiplier) and as measured by the dimethyl ether GM detector were comparable. The measured spectra could be laid on top of one another. Moreover, the optical bandpass $\Delta\hbar\omega_d$ of the dimethyl ether/MgF₂ combination had been measured at a synchrotron source¹³ and it was found to be 0.6eV. The optical bandpass of the MM1 based bandpass detector had also been measured at a

synchrotron source and it was also found to be $0.6\text{eV}^{25,26}$. The results that we present here suggest that the inference that we made in our earlier paper¹⁶, that $\Delta\hbar\omega_d=0.6\text{eV}$ for the dimethyl ether detector is incorrect. The bandpass of both the dimethyl ether detector and our MM1 based photon detector should be revised up to $(0.71\pm 0.04)\text{eV}$. To double-check this we re-analyzed the Fermi edges that we published earlier¹⁶ and found the bandpass to be $(0.71\pm 0.04)\text{eV}$. Estimates of $\Delta\hbar\omega_d$ that we recently extracted from the Fermi edges of polycrystalline indium films grown on silicon with the dimethyl ether detector are also in this range²³.

It remains to establish why our estimate of $\Delta\hbar\omega_d$ for the dimethyl ether detector ($(0.71\pm 0.04)\text{eV}$) is so much larger than the 0.6eV derived from transmission measurements¹³. We initially thought that this difference could be attributed to the asymmetric shape of the transmission function. However, the transmission function of the dimethyl ether detector is remarkably symmetric for a detector of this type. To illustrate this, we digitized the published transmission function¹³ and fitted a Gaussian function to it and found that the FWHM of the Gaussian function ($0.54 \pm 0.03\text{eV}$) was very close to the quoted FWHM (0.6eV). Consequently, we do not believe that the approximation that we have adopted in this paper, that the transmission function is symmetric, is the cause of this discrepancy. One remaining possibility is that the presence of the ethanol quench gas modifies the transmission function. This may be an opportune time to re-measure the transmission function of the dimethyl ether/ MgF_2 detector with the gas mixture that is used in a practical detector. It would be particularly interesting to see if the presence of the ethanol quench gas alters the dimethyl ether transmission function in any way.

V. DISCUSSION

The bandpass of the ethanol detector, $\Delta\hbar\omega_d=(0.37\pm 0.05)\text{eV}$, and the bandpass of the n-propanol detector, $\Delta\hbar\omega_d=(0.41\pm 0.05)\text{eV}$, are both considerably narrower than the bandpass of the dimethyl ether detector, $\Delta\hbar\omega_d=(0.71\pm 0.04)\text{eV}$ and that makes them ideally suited for studies of surface electronic structure. The bandpass of both detectors are also very competitive with solid state detectors²⁵⁻³⁴. A major advantage of building bandpass detectors with MgF_2 rather than CaF_2 or SrF_2 is that the detection energy is relatively high. Consequently, the smallest energy that the electron gun has to operate at is increased and

that makes the operation of the source considerably easier. Operating the Stoffel-Johnson source¹⁴ at 6-7eV requires the contact potential difference between the electrodes and the cathode to be carefully measured and corrected to ensure that the potentials applied to the lenses are close to the design specifications. This becomes less of a problem at higher energies.

We have very recently discovered that methanol (IP = 10.85 ± 0.02 eV⁷) can also be used as a self-quenching detection gas. This brings the total number of detection gases that can be used with the MgF₂ entrance window up to 4 and all three of the new detection gases that we have introduced in this paper, n-propanol, ethanol and methanol, are self-quenching. Moreover, if we take the bandpass of the MgF₂/methanol detector to be 75% of the difference between the high energy transmission threshold of MgF₂ and the IP of methanol (i.e. in the same proportion as the ethanol detector) then the methanol detector should have a bandpass $\Delta\hbar\omega_d \approx 0.100$ eV. This is less than half the bandpass of the iodine/SrF₂ ($\Delta\hbar\omega_d = 0.265$ eV)⁹. It is also significantly narrower than our electron beam width ($\Gamma_{\text{SOURCE}} \approx 0.220$ eV). To take advantage of this extremely narrow bandpass we will need to collect more of the photons that leave the surface. We are currently making modifications to our inverse system that will increase our solid angle of detection from $0.04(2\pi)\text{Sr} \rightarrow 0.60(2\pi)\text{Sr}$. This will help to offset the large reduction in counts produced by the narrow bandpass. With an un-monochromated electron source, the total bandpass for the methanol detector should be ≈ 0.240 eV and it could be possible to use an electron monochromator to decrease the total bandpass below this value.

Acknowledgments

This research was supported by the Natural Sciences and Engineering Research Council of Canada. We acknowledge the assistance of Gary Contant.

-
- * mclean@physics.queensu.ca; <http://nanophysics.phy.queensu.ca>
- ¹ G. Denninger, V. Dose, and H. Scheidt, *Appl. Phys.* **18**, 375 (1979).
 - ² V. Dose, *Prog. Surf. Sci.* **13**, 225 (1983).
 - ³ V. Dose, *Appl. Phys.* **14**, 117 (1977).
 - ⁴ N. Smith, *Rep. Prog. Phys.* **51**, 1227 (1988).
 - ⁵ P. D. Johnson and S. L. Hulbert, *Rev. Sci. Instrum.* **61**, 2277 (1990).
 - ⁶ D. P. Woodruff, *J. Vac. Sci. Technol. A* **1**, 1104 (1983).
 - ⁷ K. Watanabe, T. Nakayama, and J. Mottl, *J. Quant. Spectros. Transfer* **2**, 369 (1962).
 - ⁸ D. F. Heath and P. A. Sacher, *Appl. Opt.* **5**, 937 (1966).
 - ⁹ V. Dose, *Appl. Phys. A* **40**, 203 (1986).
 - ¹⁰ J. A. R. Samson, *Techniques of Vacuum Ultraviolet Spectroscopy* (John Wiley & Sons, New York, 1967).
 - ¹¹ P. M. G. Allen, P. J. Dobson, and R. G. Edgell, *Solid State Commun.* **25**, 701 (1985).
 - ¹² D. Funnemann and H. Merz, *J. Phys. E: Sci. Instrum.* **19**, 554 (1986).
 - ¹³ K. C. Prince, *Rev. Sci. Instrum.* **59**, 741 (1988).
 - ¹⁴ N. G. Stoffel and P. D. Johnson, *Nucl. Instrum. Methods* **A234**, 230 (1984).
 - ¹⁵ I. G. Hill, Ph.D. thesis, Queen's University (1997).
 - ¹⁶ I. G. Hill and A. B. McLean, *Rev. Sci. Instrum.* **69**, 261 (1998).
 - ¹⁷ I. G. Hill and A. B. McLean, *Phys. Rev. B* **56**, 15725 (1997).
 - ¹⁸ I. G. Hill and A. B. McLean, *Applied Surf. Sci.* **123/124**, 371 (1998).
 - ¹⁹ I. G. Hill and A. B. McLean, *Phys. Rev. B* **59**, 9791 (1999).
 - ²⁰ I. G. Hill and A. B. McLean, *Phys. Rev. Lett.* **82**, 2155 (1999).
 - ²¹ A. B. McLean and I. G. Hill, *Applied Surf. Sci.* **162–163**, 620 (2000).
 - ²² G. F. Knoll, *Radiation Detection and Measurement* (John Wiley & Sons, New York, 1989), 2nd ed.
 - ²³ J. Lipton-Duffin, Master's thesis, Queen's University (2001).
 - ²⁴ W. A. Royer and N. V. Smith, *Rev. Sci. Instrum.* **59**, 737 (1988).
 - ²⁵ I. Schäfer et al., *Rev. Sci. Instrum.* **58**, 710 (1987).
 - ²⁶ N. Babbe et al., *J. Phys. E* **18**, 149 (1985).

- ²⁷ R. Avci, Q. Cai, and G. Lapeyre, *Rev. Sci. Instrum.* **60**, 3643 (1989).
- ²⁸ K. Yokoyama et al., *Rev. Sci. Instrum.* **64**, 87 (1993).
- ²⁹ W. Sheils, R. Leckey, and J. Riley, *Rev. Sci. Instrum.* **64**, 1194 (1993).
- ³⁰ Y. Ueda, K. Nishihara, K. Mimura, Y. Hari, and M. Taniguchi, *Nucl. Instrum. Methods* **A330**, 140 (1993).
- ³¹ M. Finazzi, A. Bastianon, G. Chiaia, and F. Ciccacci, *Meas. Sci. Technol.* **4**, 234 (1993).
- ³² N. Sanada, M. Shimomura, and Y. Fukuda, *Rev. Sci. Instrum.* **64**, 3480 (1993).
- ³³ F. Schedin, G. Thornton, and R. Uhrberg, *Rev. Sci. Instrum.* **68**, 41 (1997).
- ³⁴ H. Namatame et al., *J. Electron. Spectr.* **80**, 393 (1996).

Table 1

Detection Gas	$\hbar\omega_d/\text{eV}$	$\Delta\hbar\omega_d/\text{eV}$	$\tau_d/\mu\text{s}$	$\tau_r/\mu\text{s}$
Ethanol	10.89 ± 0.07	0.37 ± 0.05	145 ± 10	150 ± 10
n-Propanol	10.76 ± 0.07	0.41 ± 0.05	220 ± 10	150 ± 10
Dimethyl Ether	10.60	0.71 ± 0.04	100 ± 10	125 ± 10

$\hbar\omega_d$ is the detection energy, $\Delta\hbar\omega_d$ is the FWHM energy bandpass, τ_d is the dead time and τ_r is the recovery time. The detection energy of the dimethyl ether detector was measured using a synchrotron source¹³.

Figures

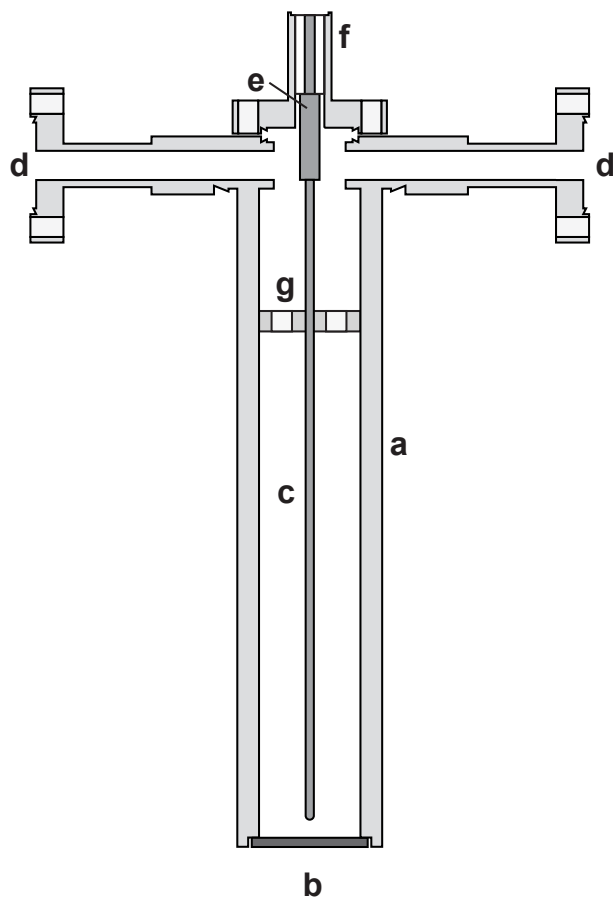


FIG. 1:

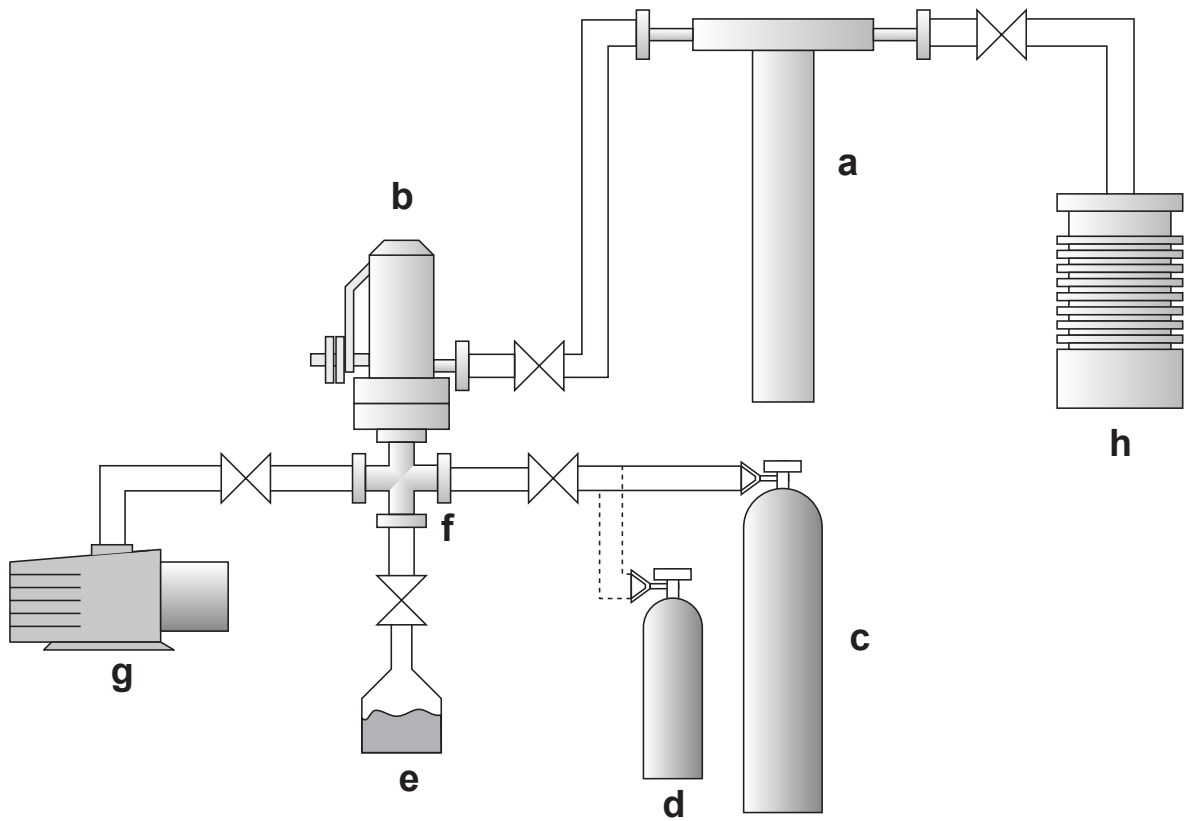


FIG. 2:

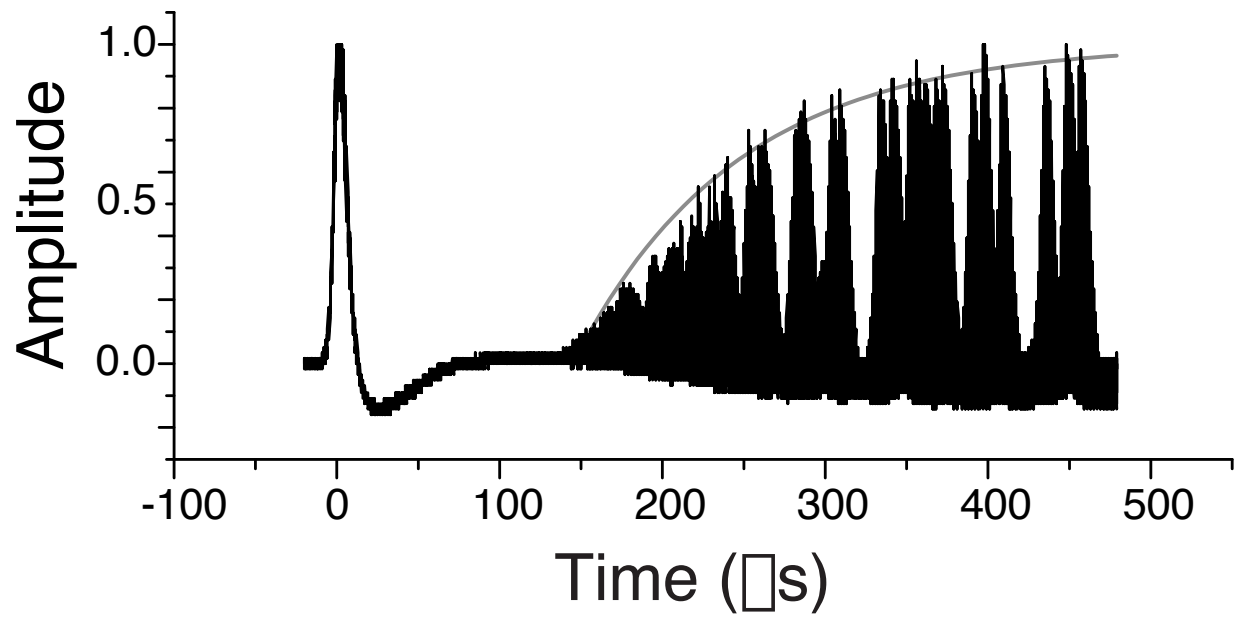


FIG. 3:

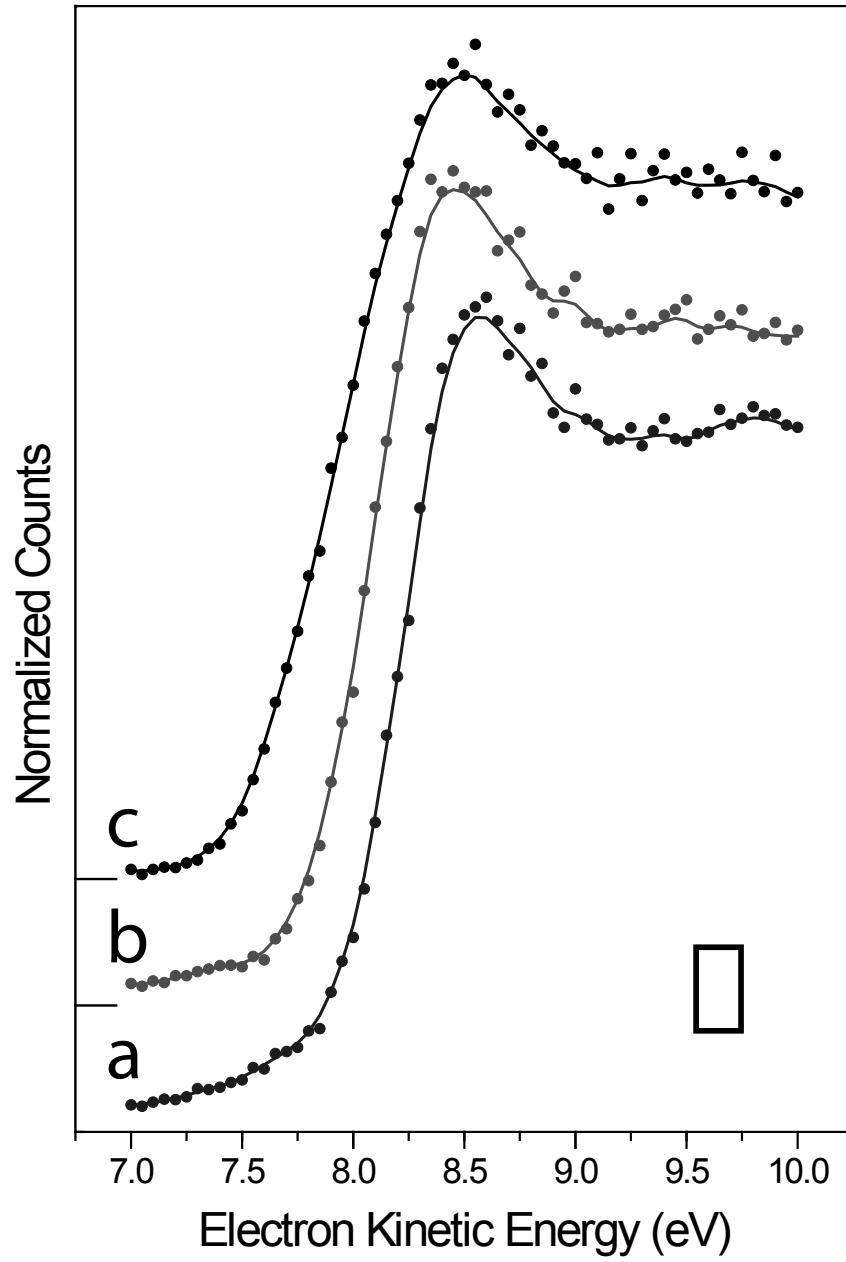


FIG. 4:

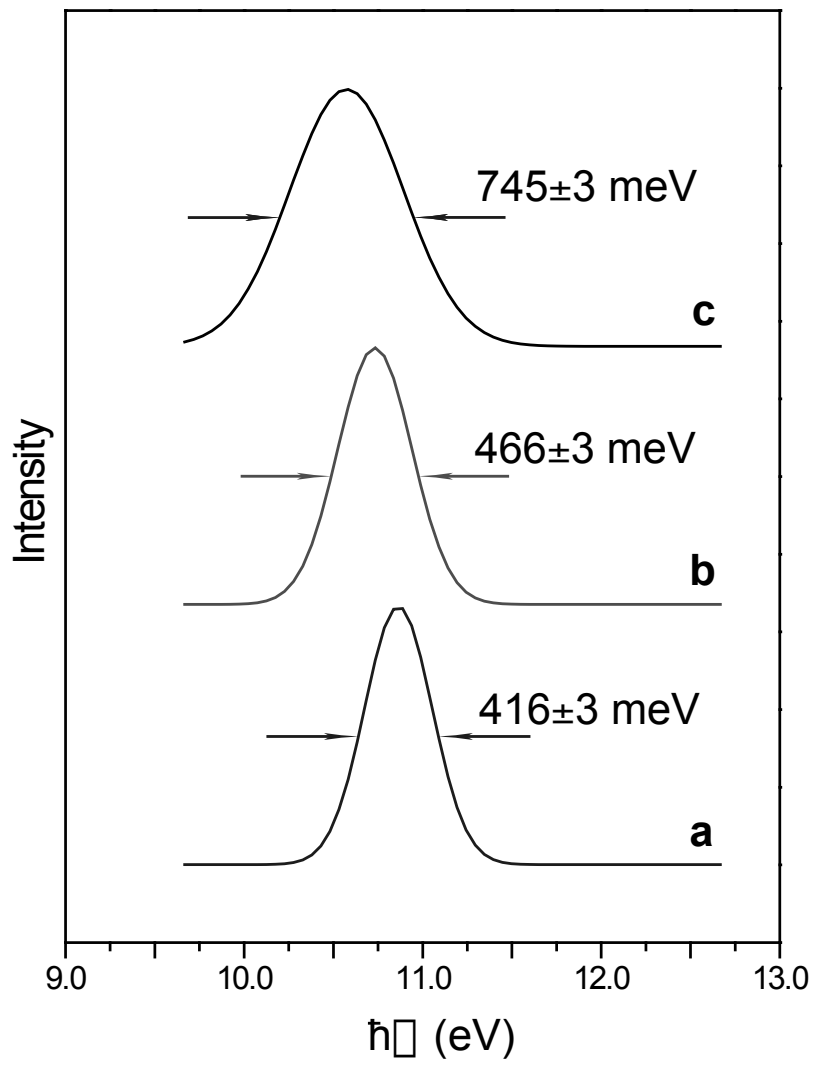


FIG. 5:

Figure Captions

Fig.1: A cross section through the stainless steel Geiger Müller tube **(a)** showing: **(b)** the MgF_2 window, **(c)** the stainless steel electrode, **(d)** the gas handling ports, **(e)** the barrel connector and **(f)** the mini-conflat high voltage SHV feedthrough, **(g)** the PTFE support spacer. The tube has an outer diameter of 1.25 inches and an inner diameter of 0.875 inches.

Fig.2: Schematic of the Geiger-Müller gas handling manifold, showing: **(a)** Geiger-Müller Tube, **(b)** Precision Leak Valve, **(c)** Argon bottle, **(d)** Dimethyl ether bottle, **(e)** Ethanol/propanol reservoir, **(f)** 4-way cross, **(g)** 2-stage rotary pump, **(h)** Turbomolecular pump.

Fig.3: The envelope of pulse height distributions from a GM tube filled with 1.15 Torr of ethanol and ≈ 100 Torr of argon multiplier gas. A non-linear least-squares fits to the recovery curve yielded a detector dead time of $\tau_d = (100 \pm 10)\mu s$ and a recovery time of $\tau_r = (125 \pm 10)\mu s$.

Fig.4: The Fermi edge of Cu(111) measured using **(a)** ethanol, **(b)** n-propanol and **(c)** dimethyl ether detectors. The edge sharpens in the sequence: **(c)** \rightarrow **(a)**. The peak close to 8.5eV is the Shockley surface state that is made visible in the normal incidence geometry by the large spread in the parallel momentum of the electron beam²⁴.

Fig.5: Resolution functions, that were obtained by fitting Gaussians to the derivative of the measured edges, plotted against photon energy: **(a)** ethanol, **(b)** n-propanol and **(c)** dimethyl ether. As the bandpass narrows, the mean detection energy moves to higher energy, as expected.